



Recurrency time entropy of brain wave rhythms as an indicator of performance on visual search tasks in schoolchildren

Artem Badarin^a, Nikita Brusinskii^b, Vadim Grubov^c, Tatiana Bukina^d , Semen Kurkin^e, Marina V. Khramova^f, and Alexander E. Hramov^g

Baltic Center for Neurotechnology and Artificial Intelligence, Immanuel Kant Baltic Federal University, 14 Alexander Nevsky Street, Kaliningrad 236016, Russia

Received 12 August 2024 / Accepted 16 September 2024

© The Author(s), under exclusive licence to EDP Sciences, Springer-Verlag GmbH Germany, part of Springer Nature 2024

Abstract This study demonstrates that the entropy of brain rhythms in the alpha and beta ranges serves as a significant indicator of the efficiency of visual information processing. We employed the method of recurrent quantitative analysis to estimate the recurrency time entropy across various EEG frequency ranges and conducted a correlation analysis to identify significant relationships between entropy and reaction time. EEG signals were collected from children aged 8–11 years while they performed visual search tasks. Our results indicate that higher entropy is associated with more efficient visual information processing.

1 Introduction

The study of the neurophysiological mechanisms underlying cognitive processes cannot be overemphasized. These studies are important both for the fundamental understanding of brain mechanisms and its healthy functioning, as well as for identifying biomarkers of various neurodegenerative diseases [1–6]. Indeed, various neurointerfaces and diagnostic systems based on the analysis of brain activity have been actively developed recently [7–12]. Additionally, areas related to neuroeducation have seen significant growth [9, 13, 14]. In particular, in our previous work [9], we proposed the open-loop neuroadaptive system for enhancing student's cognitive abilities in learning. There, the assessment of cognitive abilities was based on the concept of executive functions.

Continuing this line of research, we have focused on studying specific tasks that reflect distinct cognitive processes. One such task is visual search, which plays a key role in cognitive activity, involving such functions as attention, memory, and perception [15–18]. Visual search is the process of finding a target object among multiple distracting stimuli. Understanding the mechanisms of visual search allows us to improve the diagnosis and treatment of neurodegenerative diseases, as well as to develop more effective strategies for learning and training cognitive abilities. This is particularly relevant to cognitive development in children, as the brain is most receptive to learning in early age [19–21].

Our previous studies have shown that the variability of alpha and beta rhythms in electroencephalogram (EEG) signals during the performance of cognitive tasks is a good indicator of performance in the Bourdon test [22] and in the Sternberg working memory task [23]. Indeed, the fluctuations of alpha and beta waves reflect the processes of inhibition and excitation, and their variability is probably related to the balance of these processes, which can also affect the quality of task performance [24–26]. However, the measure proposed by us only roughly reflects the dynamic characteristics of the rhythms, not reflecting their complexity or regularity, and actually takes into

^a e-mail: badarin.a.a@mail.ru

^b e-mail: nikita@brusinskii.ru

^c e-mail: vvgrubov@gmail.com

^d e-mail: bukinatatyanav@gmail.com (corresponding author)

^e e-mail: kurkinsa@gmail.com

^f e-mail: mhramova@gmail.com

^g e-mail: aekhramov@kantiana.ru

account only the range of oscillations. Therefore, in this paper we continue to study the dynamic characteristics of wave rhythms arising in the process of cognitive task performance and investigate the complexity of these signals with recurrence quantification analysis (RQA) and entropy computation [27].

Entropy measures have recently become popular in neuroscience for detecting and quantifying variability in brain activity. For example, Quiñan Quiroga et al. [28] studied event-related potentials with wavelet entropy and found that entropy reduction correlated with responses to target stimuli, reflecting the fact that these responses are tied to a more “ordered” state than spontaneous EEG. Another work analyzed entropy characteristics in the context of cognitive load analysis, showing that an increase in load leads to a decrease in signal entropy [29]. A study of default mode network (DMN) complexity using multi-scale entropy [30] demonstrated that cognitive decline in Alzheimer’s disease is reflected in reduced signal complexity in DMN nodes. Research on the characteristics of visual attention has linked EEG signal entropy to visual attention; for example, Li et al. [31] showed that entropy in attention tasks is higher than in the resting state.

Thus, the entropy analysis of EEG signals seems to be a promising direction, especially in the field of cognitive function studies. In this regard, the aim of this work is to study the characteristics of the entropy of EEG wave rhythms in school-age children and to search for their relationship with the efficiency of visual search performance.

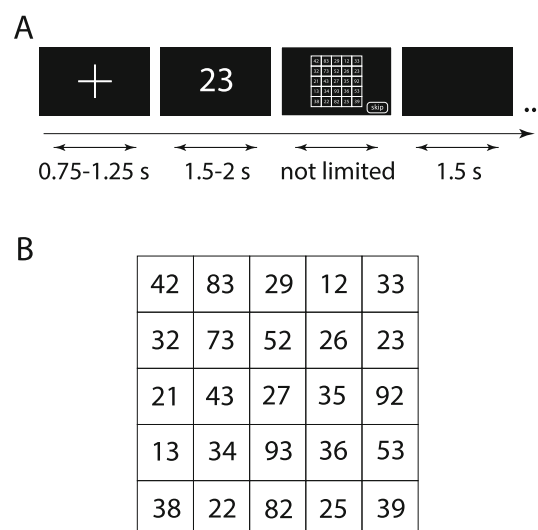
2 Materials and methods

2.1 Experimental procedure

The experimental procedure was based on the approach for assessing cognitive abilities described in our paper [9]. Here, we considered only the test for visual search assessment. The completion of this cognitive test involves solving multiple tasks of the same type. The general scheme of one task is shown in Fig. 1A. The screen is black and all information is presented with white lines and symbols to not overwhelm sight of the participant. Prior to the task, a cross appears on the screen for 0.75 to -1.25 s to attract the participant’s attention. Fluctuations in all presentation times are implemented to prevent the participant from getting used to the timings [32]. After the cross, the target number is displayed on the screen for 1.5–2 s. At this point the goal of the participant is to remember the target number. After the target, a 5×5 table of numbers is presented on the screen. Now the participant’s task is to find and indicate the target number in the table. The table remains on the screen until the participant provides an answer, i.e., the time for the task is not limited. There is an opportunity to skip a particular task by pressing the “skip” button in the bottom right. This option is implemented for the cases when the participant was unfocused or distracted and could not remember the target number. A short pause of 1.5 s follows the participant’s answer, and after it the next task begins.

The test implements two types of tables consisting of two-digit numbers. Example of table is presented in Fig. 1B. Tables of the first type are composed of numbers that contain at least one or both digits of the target number. For example, for the target number “23”, a table of the first type can include the following numbers: “53”, “21”, “32”, etc. (see Fig. 1B). In tables of the second type, all the numbers do not include any digits from the target number. For instance, for the same target number “23”, a table of the second type can include “14”, “65”, “80”, etc. The two types of tables are designed to test two different options for visual search: when the target object has

Fig. 1 (A) General scheme for visual search task; (B) example of table with two-digit numbers



similarities with other objects, and when it does not [33]. The test uses equal number of tables of the first and the second type, randomly mixed. There are 10 tasks for each type of table, resulting in a total of 20 tasks.

2.2 Data acquisition and preprocessing

An electroencephalogram (EEG) was recorded using LiveAmp (Brain Products, Germany). Recording was performed for 64 EEG channels at a sampling rate of 500 Hz. Electrodes were placed according to the international “10–10” arrangement scheme with ground electrode in “Fpz” position and reference electrode in “Fz” position. NuPrep abrasive gel and conductive SuperVisc gel were used during electrode installment to achieve low impedance ($< 10 \text{ k}\Omega$) and high quality of EEG signals.

EEG data was preprocessed in two steps. Firstly, we applied filtering. We used band-pass filter 1–40 Hz to restrict parasitic component with pronounced low and high frequencies, for instance breathing and muscle artifacts [34]. Secondly, we used a method based on independent components analysis (ICA) [35] to remove artifacts interfering with frequency range of EEG such as blinks. Preprocessing was done with the help of EEGLAB—MATLAB toolbox specifically designed for the analysis of electrophysiological signals, in particular EEG [36].

2.3 Participants

The study involved 54 students from Lyceum No. 23 in Kaliningrad, Russia. The students were of two age categories: 8–11 years old (26 participants, grades 3–4) and 10–12 years old (28 participants, grade 5). There were 34 boys and 20 girls. Two participants were excluded, since they could not complete all tasks in the experiment due to various personal reasons such as high fatigue and low involvement in the task.

The experimental study was conducted in the morning in a quiet room with sufficient natural light. Before the experiment, the student was advised to follow a healthy lifestyle for 48 h, including an 8-h night’s rest, moderate physical activity and limited caffeine consumption. Before participating in the study, the student and their parents (legal guardians) were instructed of the general design, objectives and methods of the experiment. They were allowed to ask any related questions and received comprehensive answers. After that, the parents (legal guardians) filled out and signed the informed consent form. The experimental study was conducted in accordance with the Declaration of Helsinki. The study design was approved by the Ethics Committee of Immanuel Kant Baltic Federal University (Protocol No. 32 from 04.07.2022).

2.4 Time–frequency analysis

We analyzed the EEG signals recorded during the visual search task using a continuous wavelet transform (CWT) [37]. The energy spectrum of the wavelet $E_{\Delta_f}^n$ was calculated for each EEG channel $X_n(t)$ and averaged over frequencies in each of the four ranges Δ_f : 1–4 Hz ($\Delta_f\delta$), 4–8 Hz ($\Delta_f\theta$), 8–14 Hz ($\Delta_f\alpha$), 14–30 Hz ($\Delta_f\beta$).

$$E_{\Delta_f}^n(t) = \frac{1}{\Delta_f} \int_{f \in \Delta_f} \sqrt{W_n(f, t)^2} df, \quad (1)$$

where n is the EEG channel number, $\Delta_f \in \{\Delta_f\delta, \Delta_f\theta, \Delta_f\alpha, \Delta_f\beta\}$, $W_n(f, t)$ are complex-valued wavelet coefficients calculated as [38]:

$$W_n(f, t) = \sqrt{f} \int_{t-4/f}^{t+4/f} x_n(\tau) \psi^*(f, \tau) d\tau, \quad (2)$$

where $*$ denotes complex conjugation and ψ is the mother wavelet, for which we used the Morlet wavelet, often used for the analysis of neurophysiological data [38].

2.5 Entropy

The repetition of the state of a system over time is a fundamental property of dynamical systems. To analyze such repetitions, we used RQA. Note that RQA allows to identify repetitive patterns and structures in data that may not be obvious when using traditional time series analysis methods [39]. At the same time, RQA methods are highly resistant to noise, which is extremely important for EEG data that often contain a significant amount of noise [40, 41]. RQA has previously been used, for example, to diagnose motor activity from EEG signals and

has been shown to be of high quality in classifying motor acts [39, 42], and to identify changes in event-related potentials of the brain [43].

We analyzed the dynamics of energy $E_{\Delta_f}^n$ across various frequency bands and channels. Employing the Takens theorem, we reconstructed the phase space $\Phi_{\Delta_f}^n$ for each channel and frequency band separately by embedding delayed signals into the original one [44]. To determine the embedding dimension, we utilized the false nearest neighbor algorithm for each signal $E_{\Delta_f}^n$ [45]. The delay time was estimated using an algorithm based on the analysis of average mutual information (AMI), with the time delay set to the first local minimum of the AMI [46].

To analyze the recurrence structures in the selected frequency band and channel, we created a binary recurrence matrix:

$$R_{i,j} = \begin{cases} 1 & \text{if } \|\Phi_{\Delta_f,i}^n - \Phi_{\Delta_f,j}^n\| < \varepsilon, \\ 0 & \text{otherwise,} \end{cases}$$

where $\Phi_{\Delta_f,i,j}^n = \Phi_{\Delta_f}^n(t_{i,j})$, $i, j = 1, \dots, T$, T is the whole duration of task solving. The recurrence threshold ε determines the size of the neighborhood in state space in which states are considered to be recurring.

Using the binary recurrence matrix, we estimate the recurrence time entropy (ENT)—a complexity measure based on the vertical lines in the matrix indicating recurrence times t_v ,

$$ENT = - \sum_{t_v=1}^{T_{max}} p(t_v) \ln p(t_v),$$

where $p(t_v)$ is the probability of finding a vertical line of length t_v , given by $p(t_v) = h(t_v) / \sum_{t_v} h(t_v)$, and $h(t_v)$ is the histogram of recurrence times obtained from the recurrence plot (RP). This measure effectively captures transitions between periodic and chaotic dynamics, with regular processes resulting in low ENT values and chaotic processes increasing ENT values by increasing the distribution of recurrence times.

3 Results

When analyzing RP and related measures, one should take into account that the obtained results can heavily depend on the choice of neighborhood threshold. However, the choice of this threshold is often completely arbitrary and is based on empirical assumptions or the statistical distribution of all pairwise distances [47]. In this study, we followed a different principle. We calculated the neighborhood threshold to maximize the absolute Spearman's rank correlation between ENT values and the average reaction time in the sample for each channel and frequency band. Figure 2 shows an example of the correlation dependence on the neighborhood threshold for channel TP10 in the beta range. It is clearly seen that at the parameter $\varepsilon = 0.65$, a distinct optimum is achieved.

After determining the neighborhood threshold, we proceeded to analyze the obtained correlations. A threshold value of $p < 0.005$ was used for statistical significance. We did not find statistically significant correlations in the delta and theta ranges, but we identified several significant correlations in the alpha and beta bands (see Fig. 3).

Fig. 2 Dependence of Spearman's rank correlation between the values of ENT and the average reaction time for the TP10 channel in the beta range

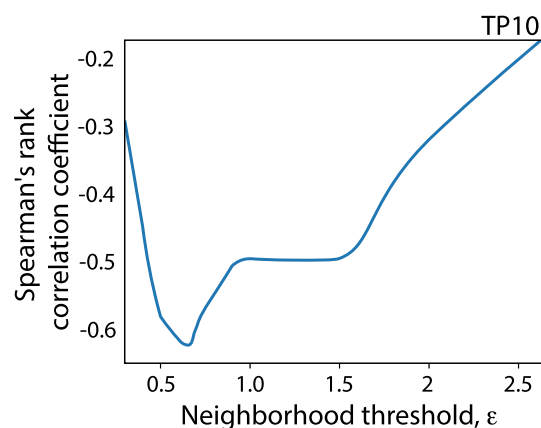
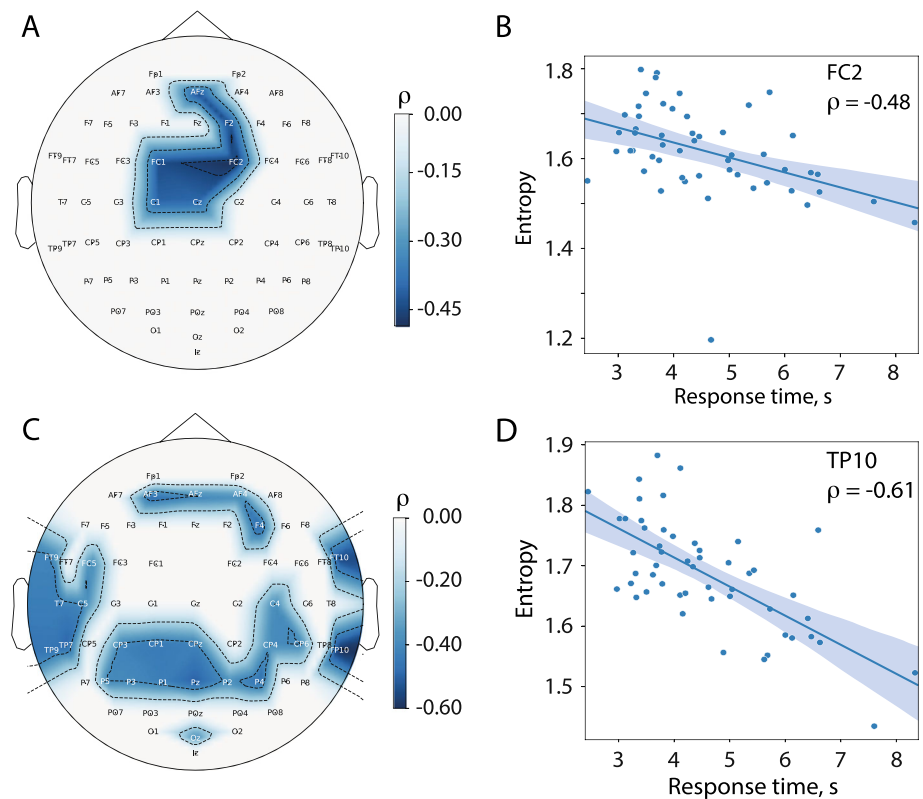


Fig. 3 (A, C)

Distributions of correlation coefficients (ρ) between response time and entropy in the alpha and beta bands, respectively, plotted on a topographic map of the scalp. The color indicates the strength and direction of the correlation. Correlation values that did not pass the significance threshold were set to zero. **(B, D)** The distribution of entropy in the alpha and beta bands, respectively, as a function of response time for the channels FC2 and TP10, where the strongest correlations were found. Data points are approximated by a regression line, and the blue area represents the 95% confidence interval



For the entropy of energy in the alpha band, a group of clustered frontocentral and midline channels (AFz, F2, FC1, FC2, C1, Cz) showed statistically significant correlation values (see Fig. 3A). The strongest correlation was observed in channel FC2 ($\rho = -0.48$, see Fig. 3B).

Figure 3A shows a topographic map demonstrating the scalp distribution of the correlation coefficients (ρ) between alpha-band entropy and reaction time. The color scale ranges from 0 to -0.48 , indicating the strength and direction of the correlation. Thus, the significant negative correlations are observed predominantly in the frontocentral and midline regions. Note, that here and below, the correlation values that did not pass the significance threshold were set to zero. Figure 3B shows the entropy distribution as a function of response time for channel FC2, where the strongest correlation was found. The data points are fitted with a regression line, and the blue area represents the 95% confidence interval. The negative slope of the regression line indicates that higher entropy in the alpha band is associated with shorter response times.

For entropy in the beta band, a greater number of statistically significant correlations were observed. The emerging pattern on the topogram was close to symmetrical. Significant channels in the frontal lobe included AF3, AFz, AF4, F4; in the central and parietal lobes—CP3, CP1, CPz, CP4, CP6, C4, P5, P3, P1, Pz, P2, P4; in the left temporal lobe—FT9, FC5, T7, C5, TP9, TP7; in the right temporal lobe—FT10, TP10; and in the occipital lobe—Oz (see Fig. 3C). The strongest correlation was observed in channel TP10 ($\rho = -0.61$, see Fig. 3D).

Figure 3C shows a topographic map of the scalp distribution of the correlation coefficients (ρ) between beta-band entropy and reaction time. The color scale ranges from 0 to -0.61 , indicating the strength and direction of the correlation. Significant negative correlations are observed predominantly in the frontal, central, parietal, left temporal, and right temporal lobes. Figure 3D shows the entropy distribution in the beta band as a function of response time for channel TP10, where the strongest correlation was found. The data points are fitted with a regression line, and the blue area represents the 95% confidence interval. The negative slope of the regression line indicates that the higher entropy in the beta band is associated with shorter response times.

4 Discussion

In this paper, the neurophysiological correlates of performing the visual search task in middle-aged schoolchildren are investigated. The main goal was to identify the relationship between the entropy characteristics of the brain rhythms energy and the effectiveness of the task. We used RQA to analyze energy entropy in various EEG frequency ranges and performed a correlation analysis to identify significant relationships between entropy and reaction time.

We found many statistically significant correlations between reaction time in visual search tasks and entropy in the alpha and beta ranges. For the alpha rhythm range, significant correlations were observed in the dorsolateral prefrontal cortex (AFz), premotor cortex (FC2, FC1), frontal eye fields (F2), and somatosensory association cortex (C1, Cz) regions. The entropy of beta rhythm energy correlated with a larger group of channels in the dorsolateral prefrontal cortex (AF3, AF4, AFz), frontal eye fields (F4), temporal lobe (FT9, TP9, FT10, TP10, T7, TP7, C5), Broca's area (FC5), parietal lobe (CP4, CP6, C4, P4, P1, P2, Pz, P3, P5, CPz, CP1, CP3), and primary visual cortex (Oz).

The results obtained are in good agreement with known data on the processing of visual information [48]. Visual information processing begins in the primary visual cortex (V1) and continues along two main pathways: ventral and dorsal [48, 49]. The ventral pathway extends into the temporal lobe and is responsible for object recognition. The dorsal pathway leads to the parietal and prefrontal cortex and is responsible for visually guided movements and attention control. Additionally, for each ascending connection, there is a corresponding descending connection that carries information about the behavioral context [49]. Furthermore, it has been shown that visual processing is closely linked to a model of frequency-specific directional interareal influences. In this model, top-down processing is primarily carried out through the synchronization of alpha and beta frequency ranges [50–52].

Thus, our results indicate that the entropy of brain rhythms reflects the frequency and regional characteristics of visual information processing. High entropy in the alpha and beta ranges is associated with more efficient processing and indicates increased complexity in the recorded signals. This complexity is possibly the result of a dynamic reorganization of neural networks and the involvement of various groups of neurons that adapt to new contexts, which contributes to more efficient information processing.

The multiple correlations found indicate that entropy can serve as an objective marker of task performance for brain-computer interfaces. We have demonstrated that the entropy of brain rhythms is closely related to task performance effectiveness. High entropy, associated with efficient information processing, can be utilized to develop advanced brain-computer interfaces that better adapt to individual user characteristics and enhance the efficiency of brain-computer interaction [53, 54].

This study has several limitations that must be acknowledged, as they may impact the generalizability of the findings. The primary limitation is the relatively small sample size, which may reduce the statistical power and restrict the broader applicability of the results. Furthermore, the sample was limited to school-aged children (8–12 years), which narrows the scope of extrapolating the findings to other age groups.

5 Conclusions

Our study demonstrates that the entropy of brain rhythms in the alpha and beta ranges is an important indicator of the effectiveness of visual information processing. By analyzing the EEG signals of children performing visual search tasks, we identified key correlations between entropy and reaction time, with high entropy indicating more efficient data processing.

These findings are valuable for the development of brain-computer interfaces, since the detected biomarker can be used as an objective indicator of the effectiveness of the task.

Thus, our results contribute to the understanding of the neurophysiological mechanisms underlying the processing of visual information. At the same time, future studies could further investigate the found correlations with respect to various age groups and tasks in order to generalize the results and increase the applicability of entropy indicators.

Acknowledgements This work was supported by the Academic Leadership Program “Priority-2030” of Immanuel Kant Baltic Federal University of Ministry of Science and Education of Russian Federation.

Data availability The data presented in this study are available on request from the corresponding author.

References

1. A. Horvath, A. Szucs, G. Csukly, A. Sakovics, G. Stefanics, A. Kamondi, Eeg and erp biomarkers of Alzheimer's disease: a critical review. *Front. Biosci. (Landmark Ed)* **23**, 183–220 (2018)
2. A.E. Hramov, V. Grubov, A. Badarin, V.A. Maksimenko, A.N. Pisarchik, Functional near-infrared spectroscopy for the classification of motor-related brain activity on the sensor-level. *Sensors* **20**(8), 2362 (2020)
3. P.M. Rossini, R. Di Iorio, F. Vecchio, M. Anfossi, C. Babiloni, M. Bozzali et al., Early diagnosis of Alzheimer's disease: the role of biomarkers including advanced eeg signal analysis report from the ifcn-sponsored panel of experts. *Clin. Neurophysiol.* **131**(6), 1287–1310 (2020)

4. G. Guyo, A. Pavlov, E. Pitsik, N. Frolov, A. Badarin, V. Grubov et al., Cumulant analysis in wavelet space for studying effects of aging on electrical activity of the brain. *Chaos Solitons Fract.* **158**, 112038 (2022)
5. A. Badarin, V. Antipov, V. Grubov, N. Grigorev, A. Savosenkov, A. Udoratina et al., Psychophysiological parameters predict the performance of naive subjects in sport shooting training. *Sensors* **23**(6), 3160 (2023)
6. O.E. Karpov, E.N. Pitsik, S.A. Kurkin, V.A. Maksimenko, A.V. Gusev, N.N. Shusharina et al., Analysis of publication activity and research trends in the field of ai medical applications: network approach. *Int. J. Environ. Res. Public Health* **20**(7), 5335 (2023)
7. V. Khorev, S. Kurkin, A. Badarin, V. Antipov, E. Pitsik, A. Andreev et al., Review on the use of brain computer interface rehabilitation methods for treating mental and neurological conditions. *J. Integr. Neurosci.* **23**(7), 125 (2024)
8. M.L. Vicchiotti, F.M. Ramos, L.E. Betting, A.S. Campanharo, Computational methods of eeg signals analysis for Alzheimer's disease classification. *Sci. Rep.* **13**(1), 8184 (2023)
9. V.V. Grubov, M.V. Khramova, S. Goman, A.A. Badarin, S.A. Kurkin, D.A. Andrikov et al., Open-loop neuroadaptive system for enhancing student's cognitive abilities in learning. *IEEE Access* **12**, 49034 (2024)
10. D. Stoyanov, V. Khorev, R. Paunova, S. Kandilarova, D. Simeonova, A. Badarin et al., Resting-state functional connectivity impairment in patients with major depressive episode. *Int. J. Environ. Res. Public Health* **19**(21), 14045 (2022)
11. A.V. Andreev, S.A. Kurkin, D. Stoyanov, A.A. Badarin, R. Paunova, A.E. Hramov, Toward interpretability of machine learning methods for the classification of patients with major depressive disorder based on functional network measures. *Chaos Interdiscip. J. Nonlinear Sci.* **33**, 6 (2023)
12. A.N. Pisarchik, A.V. Andreev, S.A. Kurkin, D. Stoyanov, A.A. Badarin, R. Paunova et al., Topology switching during window thresholding fmri-based functional networks of patients with major depressive disorder: Consensus network approach. *Chaos Interdiscip. J. Nonlinear Sci.* **33**, 9 (2023)
13. B. Maxwell, E. Racine, The ethics of neuroeducation: Research, practice and policy. *Neuroethics* **5**(2), 101–103 (2012)
14. J. Jolles, D.D. Jolles, On neuroeducation: Why and how to improve neuroscientific literacy in educational professionals. *Front. Psychol.* **12**, 752151 (2021)
15. R. Dell'Acqua, P. Sessa, P. Toffanin, R. Luria, P. Jolicœur, Orienting attention to objects in visual short-term memory. *Neuropsychologia* **48**(2), 419–428 (2010)
16. U. Leonards, S. Sunaert, P. Van Hecke, G.A. Orban, Attention mechanisms in visual search-an fmri study. *J. Cogn. Neurosci.* **12**(Supplement 2), 61–75 (2000)
17. G. Kong, D. Fougny, Visual search within working memory. *J. Exp. Psychol. Gen.* **148**(10), 1688 (2019)
18. N. Brusinsky, A. Badarin, A. Andreev, V. Antipov, S. Kurkin, A. Hramov, Analysis of the cognitive load in sternberg's problem in an eye-tracker study. *Bull. Russ. Acad. Sci. Phys.* **87**(1), 105–107 (2023)
19. T.T. Brown, T.L. Jernigan, Brain development during the preschool years. *Neuropsychol. Rev.* **22**, 313–333 (2012)
20. S. Frangou, A. Modabbernia, S.C. Williams, E. Papachristou, G.E. Doucet, I. Agartz et al., Cortical thickness across the lifespan: Data from 17,075 healthy individuals aged 3–90 years. *Hum. Brain Mapp.* **43**(1), 431–451 (2022)
21. V.A. Anderson, G. Lajoie, Development of memory and learning skills in school-aged children: A neuropsychological perspective. *Appl. Neuropsychol.* **3**(3–4), 128–139 (1996)
22. N. Smirnov, A. Badarin, S. Kurkin, A. Hramov, A new electroencephalography marker of cognitive task performance. *Bull. Russ. Acad. Sci. Phys.* **87**(1), 108–111 (2023)
23. N. Brusinsky, A. Badarin, A. Andreev, V. Antipov, S. Kurkin, Dynamics of the brain's wave rhythms predict the speed of performing cognitive tasks. *Bull. Russ. Acad. Sci. Phys.* **88**(1), 138–141 (2024)
24. K.E. Mathewson, A. Lleras, D.M. Beck, M. Fabiani, T. Ro, G. Gratton, Pulsed out of awareness: Eeg alpha oscillations represent a pulsed-inhibition of ongoing cortical processing. *Front. Psychol.* **2**, 99 (2011)
25. A. Stolk, L. Brinkman, M.J. Vansteensel, E. Aarnoutse, F.S. Leijten, C.H. Dijkerman et al., Electrocorticographic dissociation of alpha and beta rhythmic activity in the human sensorimotor system. *Elife* **8**, e48065 (2019)
26. M.V. Khramova, A.K. Kuc, V.A. Maksimenko, N.S. Frolov, V.V. Grubov, S.A. Kurkin et al., Monitoring the cortical activity of children and adults during cognitive task completion. *Sensors* **21**(18), 6021 (2021)
27. C.L. Webber, N. Marwan, Recurrence quantification analysis. *Theory Best Pract.* **426**, 8 (2015)
28. R. Quiñan Quiroga, O.A. Rosso, E. Başar, M. Schürmann, Wavelet entropy in event-related potentials: a new method shows ordering of eeg oscillations. *Biol. Cybern.* **84**(4), 291–299 (2001)
29. P. Zarjam, J. Epps, N.H. Lovell, Characterizing mental load in an arithmetic task using entropy-based features, in *2012 11th International Conference on Information Science. (IEEE, Signal Processing and their Applications (ISSPA), 2012)*, pp.199–204
30. M. Grieder, D.J. Wang, T. Dierks, L.O. Wahlund, K. Jann, Default mode network complexity and cognitive decline in mild alzheimer's disease. *Front. Neurosci.* **12**, 770 (2018)
31. W. Li, D. Ming, R. Xu, H. Ding, H. Qi, B. Wan, Research on visual attention classification based on eeg entropy parameters, in *World Congress on Medical Physics and Biomedical Engineering May 26–31, 2012.* (Beijing, China, Springer, 2013), pp.1553–1556
32. G. Derosi, N. Farrugia, S. Perrey, T. Ward, K. Torre, Expectations induced by natural-like temporal fluctuations are independent of attention decrement: evidence from behavior and early visual evoked potentials. *Neuroimage* **104**, 278–286 (2015). <https://doi.org/10.1016/j.neuroimage.2014.09.015>
33. J.E. Hoffman, A two-stage model of visual search. *Percept. Psychophys.* **25**(4), 319–327 (1979). <https://doi.org/10.3758/BF03198811>

34. M.M.N. Mannan, M.A. Kamran, M.Y. Jeong, Identification and removal of physiological artifacts from electroencephalogram signals: A review. *IEEE Access* **6**, 30630–30652 (2018). <https://doi.org/10.1109/ACCESS.2018.2842082>
35. J. Iriarte, E. Urrestarazu, M. Valencia, M. Alegre, A. Malanda, C. Viteri et al., Independent component analysis as a tool to eliminate artifacts in eeg: a quantitative study. *J. Clin. Neurophysiol.* **20**(4), 249–257 (2003). <https://doi.org/10.1097/00004691-200307000-00004>
36. A. Delorme, S. Makeig, Eeglab: an open source toolbox for analysis of single-trial eeg dynamics including independent component analysis. *J. Neurosci. Methods* **134**(1), 9–21 (2004). <https://doi.org/10.1016/j.jneumeth.2003.10.009>
37. A.N. Pavlov, A.E. Hramov, A.A. Koronovskii, E.Y. Sitnikova, V.A. Makarov, A.A. Ovchinnikov, Wavelet analysis in neurodynamics. *Phys. Usp.* **55**(9), 845 (2012)
38. A.E. Hramov, A.A. Koronovskii, V.A. Makarov, V.A. Maksimenko, A.N. Pavlov, E. Sitnikova, *Wavelets in Neuroscience* (Springer Nature, Berlin, 2021)
39. E. Pitsik, N. Frolov, K. Hauke Kraemer, V. Grubov, V. Maksimenko, J. Kurths et al., Motor execution reduces eeg signals complexity: Recurrence quantification analysis study. *Chaos Interdiscip J Nonlinear Sci* **30**, 2 (2020)
40. M. Thiel, M.C. Romano, J. Kurths, R. Meucci, E. Allaria, F.T. Arecchi, Influence of observational noise on the recurrence quantification analysis. *Phys. D* **171**(3), 138–152 (2002)
41. C.J. Hasson, R.E. Van Emmerik, G.E. Caldwell, J.M. Haddad, J.L. Gagnon, J. Hamill, Influence of embedding parameters and noise in center of pressure recurrence quantification analysis. *Gait Post.* **27**(3), 416–422 (2008)
42. E.N. Pitsik, Recurrence quantification analysis provides the link between age-related decline in motor brain response and complexity of the baseline eeg. *Izvestija VUZov Prikladnaja Nelineynaja Dinamika* **29**(3), 386–397 (2021)
43. N. Frolov, E. Pitsik, V. Maksimenko, A. Hramov, Applying recurrence time entropy to identify changes in event-related potentials. *Eur. Phys. J. Spec. Top.* **232**(1), 161–168 (2023)
44. N.H. Packard, J.P. Crutchfield, J.D. Farmer, R.S. Shaw, Geometry from a time series. *Phys. Rev. Lett.* **45**(9), 712 (1980)
45. C. Rhodes, M. Morari, False-nearest-neighbors algorithm and noise-corrupted time series. *Phys. Rev. E* **55**(5), 6162 (1997)
46. S. Wallot, D. Mønster, Calculation of average mutual information (ami) and false-nearest neighbors (fnn) for the estimation of embedding parameters of multidimensional time series in matlab. *Front. Psychol.* **9**, 1679 (2018)
47. K.H. Kraemer, R.V. Donner, J. Heitzig, N. Marwan, Recurrence threshold selection for obtaining robust recurrence characteristics in different embedding dimensions. *Chaos Interdiscip. J. Nonlinear Sci.* **28**, 8 (2018)
48. C.D. Gilbert, W. Li, Top-down influences on visual processing. *Nat. Rev. Neurosci.* **14**(5), 350–363 (2013)
49. K. Zipser, V.A. Lamme, P.H. Schiller, Contextual modulation in primary visual cortex. *J. Neurosci.* **16**(22), 7376–7389 (1996)
50. C.G. Richter, W.H. Thompson, C.A. Bosman, P. Fries, Top-down beta enhances bottom-up gamma. *J. Neurosci.* **37**(28), 6698–6711 (2017)
51. G. Michalareas, J. Vezoli, S. Van Pelt, J.M. Schoffelen, H. Kennedy, P. Fries, Alpha-beta and gamma rhythms subserve feedback and feedforward influences among human visual cortical areas. *Neuron* **89**(2), 384–397 (2016)
52. T. Van Kerkoerle, M.W. Self, B. Dagnino, M.A. Gariel-Mathis, J. Poort, C. Van Der Togt et al., Alpha and gamma oscillations characterize feedback and feedforward processing in monkey visual cortex. *Proc. Natl. Acad. Sci.* **111**(40), 14332–14341 (2014)
53. A.E. Hramov, V.A. Maksimenko, A.N. Pisarchik, Physical principles of brain–computer interfaces and their applications for rehabilitation, robotics and control of human brain states. *Phys. Rep.* **918**, 1–133 (2021)
54. B. He, H. Yuan, J. Meng, S. Gao, Brain–computer interfaces. *Neural Eng.* **2**, 131–183 (2020)

Springer Nature or its licensor (e.g. a society or other partner) holds exclusive rights to this article under a publishing agreement with the author(s) or other rightsholder(s); author self-archiving of the accepted manuscript version of this article is solely governed by the terms of such publishing agreement and applicable law.